The lateral periaqueductal gray and its role in controlling predatory hunting and social defense.

Authors: Ignacio Javier Marín-Blasco, Miguel José Rangel Jr., Marcus Vinicius C. Baldo, Simone Cristina Motta, Lisa Stowers, Newton Sabino Canteras.

Supplementary data and material.

S1. c-*fos* mRNA and Fos protein temporal dynamics in response to IP and SD.

To determine the optimum sacrificing time points, we quantified the number of Fos protein and c-*fos* mRNA positive neurons in LPAG at different time points after IP and SD. To differentiate neuronal populations in LPAG responding to insect predation (IP) and social defeat (SD), we exposed animals first to IP and subsequently to SD, particularly considering that exposure to a stressing stimulus such as SD would affect animals' motivation for hunting. The aim of this temporal profile was to find the best sacrificing time for animals exposed sequentially to IP and SD. Therefore, we performed the c-*fos* mRNA and Fos protein temporal dynamics to determine the time points when would have the maximum Fos protein expression with imperceptible levels of c-*fos* mRNA in response to the IP (the first stimulus), and optimum c-*fos* mRNA levels with reduced levels of Fos protein in response to the SD (the second stimulus). 2 hours after the set of IP, we found maximum levels of Fos protein levels and imperceptible c-*fos* mRNA signal; and 20 minutes after to the set of SD, we obtained maximum c-*fos* mRNA levels (Figure S1). However, low but perceptible synthesized Fos protein emerged at this time point in response to SD (Figure S1). Thus, we decided to shorten this time point, and sacrificed the animals 15 minutes after the set of SD when c-*fos* mRNA levels are close to the maximum, and less significant Fos protein levels were detected.

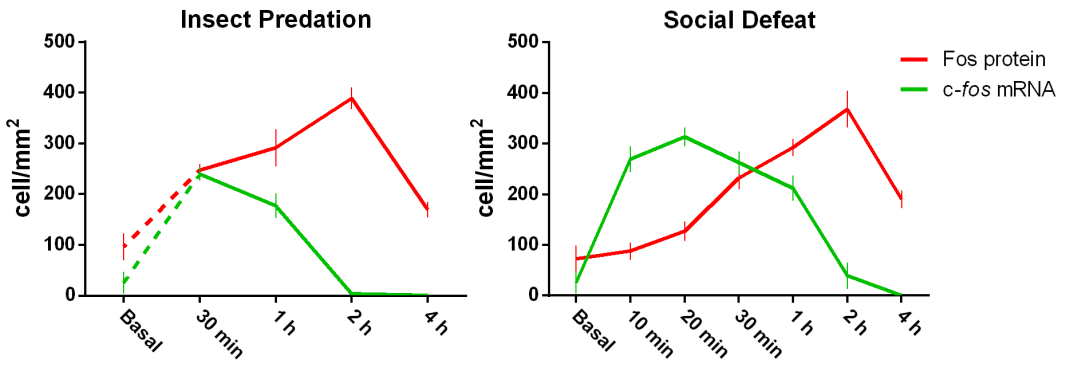

Supplementary Figure 1. c-*fos* mRNA and Fos protein temporal dynamics in response to IP and SD. Curves representing the c-*fos* mRNA and Fos protein temporal dynamics in response to IP and SD. C57BL/6J mice (n = 47) were used to determine the c-*fos* mRNA and Fos protein temporal dynamics in response to IP and SD. To this end, animals were sacrificed at basal time (n = 3), 30 min (n = 4), 1 hour (n = 4), 2 hours (n = 4) and 4 hours (n = 4) after the set of IP; and at basal time (n = 4), 10 min (n = 4), 20 min (n = 4), 30 min (n = 4), 1 hour (n = 4), 2 hours (n = 4) and 4 hours (n = 4) after the set of SD. Values expressed as means ± SEM of cells per mm^2.

S2. Descending projections of the LPAG SD responsive neurons.

According to our results, descending pathways from the LPAG to the brainstem are likely to be involved in controlling escape responses during SD. Here, we provide a comprehensive view on brainstem projections of the LPAG SD-responding neurons. Fos DD-Cre mice received injections in the LPAG of a Cre-dependent adeno-associated viral vector (AAV) expressing an EYFP reporter (AAV5-hSyn-DIO-EYFP) for tracing the projections of neurons responsive to SD. From the injection site, fibers course caudally through the periaqueductal gray and provide a dense terminal field in the ventrolateral PAG (Fig S2 A). Part of these fibers continues caudally to the pontine central gray, where labeled terminals were found in the locus coeruleus, Barrington's nucleus, lateral dorsal tegmental nucleus (Fig S2 B), and nucleus prepositus (Fig S2 C). Part of the fibers coursing through the PAG take a lateral course and project to the cuneiform nucleus (Fig S2 A) and may continue caudally to provide a sparse projection to the parabrachial nucleus (Fig S2 B) or take a ventral course to project to several fields in the reticular core. In the reticular core, particularly dense terminal fields were found in the caudal

part of the pontine reticular nucleus (Fig S2 A, B) and magnocellular reticular nucleus (Fig S2 B, C). In contrast, the gigantocellular and intermediate reticular nuclei contained a less dense projection field (Fig S2 C).

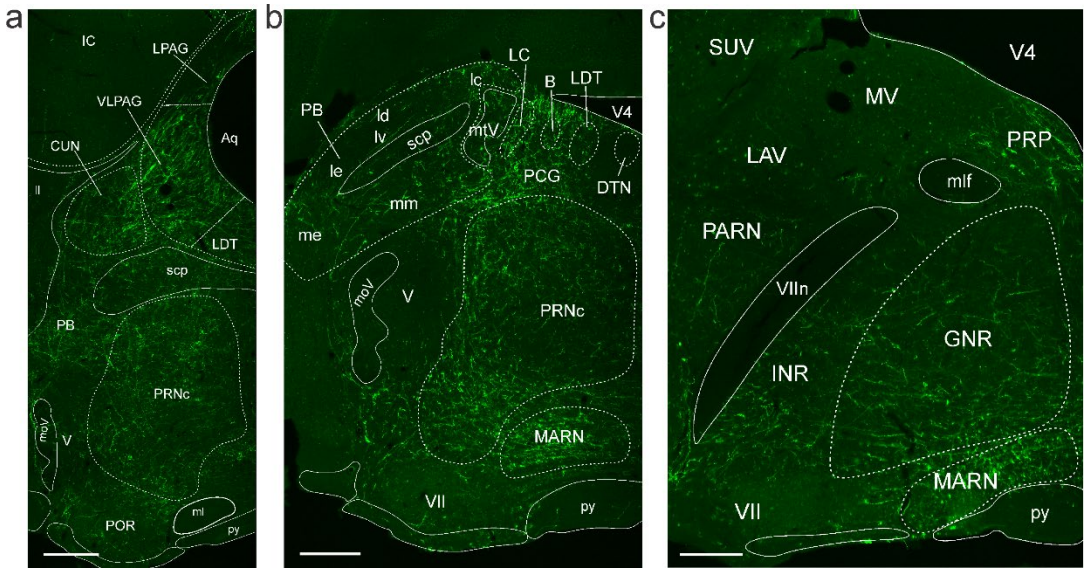

Supplementary Figure 2. Projections to the brainstem from LPAG EYFP expressing neurons activated during SD. Fluorescence photomicrographs showing the distribution of projection to the brainstem from LPAG EYFP expressing neurons activated during SD. Abbreviations: Aq - central aqueduct; B - Barrington's nucleus; CUN - cuneiform nucleus; DTN - dorsal tegmental nucleus; GNR - gigantocellular reticular nucleus; IC - inferior colliculus; INR - intermediate reticular nucleus; LAV - lateral vestibular nucleus; LC - locus ceruleus; LDT - lateral dorsal tegmental nucleus; LPAG - periaquectudal gray, lateral part; MARN - magnocellular reticular nucleus; ml - medial lemniscus; mlf - medial longitudinal fascicle; moV - motor root of the trigeminal nerve; MV - medial vestibular nucleus; PARN - parvicellular reticular nucleus; PB - parabrachial nucleus, lc – central lateral part, ld – dorsal lateral part, lv – ventral lateral part, le – external lateral part, me – external medial part, mm – medial medial part; PCG - pontine central gray; POR - superior olivary complex; PRNc - pontine reticular nucleus, caudal part; PRP - nucleus prepositus; py – pyramid; scp - superior cerebelar pedunculus; SUV - superior vestibular nucleus; V - motor nucleus of trigeminal; V4 - fourth ventricle; VII - facial motor nucleus; VIIn - facial nerve; VLPAG - periaquectudal gray, ventral lateral part. Scale bars, A - 400 µm, B – 200 µm, C – 100 µm.

S3. Phenotypic characterization of the LPAG neurons activated in the SD and IP.

To characterize the GABAergic or glutamatergic nature of LPAG neurons activated during IP and SD, we applied an IF-FISH double labeling for Fos protein and mRNAs for VGAT and VGLUT2. The results showed that the vast majority of LPAG neurons activated during IP and SD co-expressed *VGLUT2*mRNA, and just an exceedingly small number was *VGAT* mRNA

positive (Figure S3). Notably, Group SD presented a lower number of Fos/*VGLUT2* mRNA neurons when compared to IP group ($p < 0.01$) (Figure S3E). The present results are in line with previous observations showing that the LPAG contains mostly glutamatergic neurons (Lein et al. 2007) and support the idea that LPAG neurons activated during SD and IP should provide glutamatergic projections to their projection target

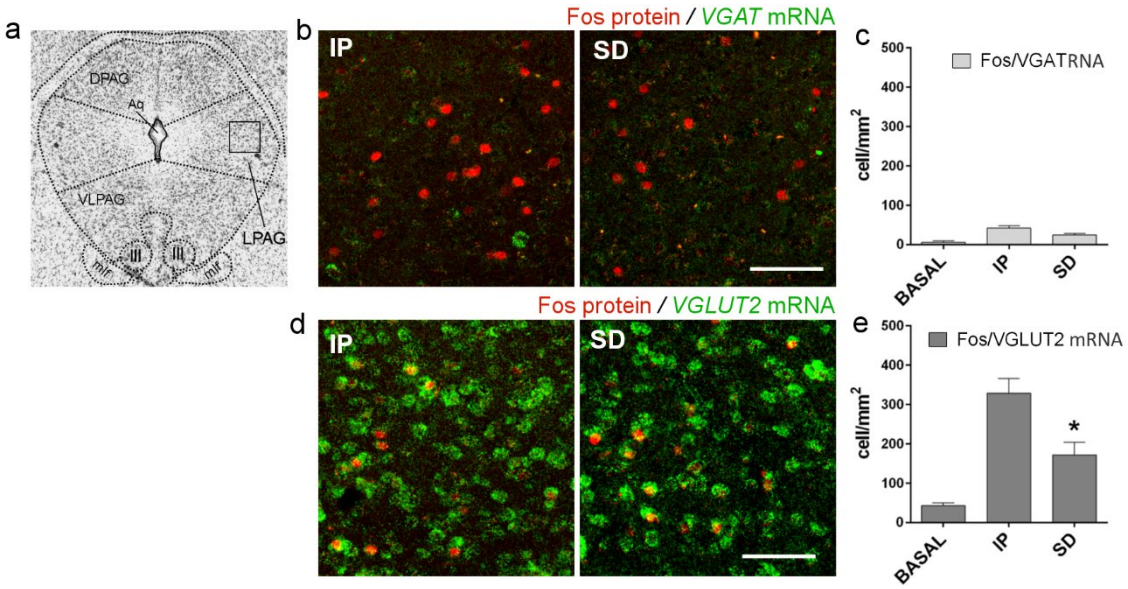

Supplementary Figure 3. Analysis of the GABAergic and glutamatergic nature of LPAG neurons recruited in response to predatory hunting and social defensive behavior. a. Photomicrograph of a representative transverse thionin-stained section of the LPAG at the level of the oculomotor nucleus (III). Square-delineated region indicates the approximate location of higher magnification fluorescence photomicrographs showing FOS / VGAT and VGLUT2 mRNAs double labeling in (B) and (D). Abbreviations: Aq - central aqueduct; III - oculomotor nucleus; LPAG - periaquectudal gray, lateral part; mlf - medial longitudinal fascicle; VLPAG - periaquectudal gray, ventral lateral part.

b. Representative fluorescence photomicrographs illustrating *Fos protein/VGAT* mRNA double labeling in LPAG of animals exposed to IP and SD. Fos protein positive cells are labeled in red (Alexa 594) and *VGAT* mRNA positive cells are labeled in green (FITC). Scale bar, 75 µm.

c. Median values of the density of Fos protein/VGAT mRNA double labeled cells in the BASAL ($n = 3$), IP ($n = 6$), and SD ($n = 6$) groups.

d. Representative fluorescence photomicrographs illustrating *Fos protein/VGULT2* mRNA double labeling in LPAG of animals exposed to IP and SD. Fos protein positive cells are labeled in red (Alexa 594) and *VGLUT2* mRNA positive cells are labeled in green (FITC). Scale bar, 75 µm.

e. Median values of the density of Fos/VGLUT2mRNA double labeled cells in the BASAL ($n = 3$), IP ($n = 6$), and SD ($n = 6$) groups. GzLM analysis of the number of Fos/*VGLUT2* mRNA neurons showed a significant effect of group factor (groups Basal, IP, and SD) [$\chi^2(2) = 44.83$, $p < 0.001$]. * indicates significant differences in *Fos protein / VGLUT2* mRNA neurons in IP versus SD group ($p < 0.01$). Data are reported as mean ± SEM. See Online Methods for detailed statistics.

S4. Videos – Functional analysis of neuronal populations in LPAG activated by IP and SD. Videos of Fos DD-Cre mice expressing inhibitory DREADD in LPAG neurons activated during IP or SD tested during prey hunting (saline-treated - Fos DDCre IP Saline; and CNO-treated - Fos DDCre IP CNO) and social defeat (saline-treated - Fos DDCre SD Saline; and CNO-treated - Fos DDCre SD CNO).

S5. Videos – Functional analysis of LHA-projecting LPAG terminals during IP and SD. Videos of C57BL/6 mice expressing eArch3.0 in LPAG projecting fibers to the LHA that receive photoinhibition during prey hunting (Laser Off – WT IP Laser off and Laser On – WT IP Laser on).

S6. Videos – Functional role of LHA^{GABA} neurons on predatory hunting. Videos comparing VGAT-IRES-Cre mice expressing inhibitory DREADD or EYFP (control group) in LHA^{GABA} neurons tested during prey hunting (saline-treated – vGAT LHA IP Saline; and CNO-treated – vGAT LHA IP CNO).